From Phage Display to Dendrimer Display: Insights into Multivalent Binding

Maartje M. C. Bastings,[†,‡] Brett A. Helms,[‡] Ingrid van Baal,[‡] Tilman M. Hackeng,[∥] Maarten Merkx,[‡] and E. W. Meijer*[,†,‡,§]

[†]Institute for Complex Molecular Systems, [‡]Laboratory of Chemical Biology, and [§]Laboratory of Macromolecular and Organic Chemistry, Eindhoven University of Technology, P.O. Box 513, 5600 MB Eindhoven, The Netherlands
[∥]Cardiovascular Research Institute Maastricht (CARIM), University Maastricht, P.O. Box 616, 6229 ER Maastricht, The Netherlands

Ⓢ *Supporting Information*

ABSTRACT: Phage display is widely used for the selection of target-specific peptide sequences. Presentation of phage peptides on a multivalent platform can be used to (partially) restore the binding affinity. Here, we present a detailed analysis of the effects of valency, linker choice, and receptor density on binding affinity of a multivalent architecture, using streptavidin (SA) as model multivalent receptor. For surfaces with low receptor densities, the SA binding affinity of multivalent dendritic phage peptide constructs increases over 2 orders of magnitude over the monovalent species (e.g., $K_{d,mono} = 120$ μM vs $K_{d,tetra} = 1$ μM), consistent with previous work. However, the affinity of the SA-binding phage presenting the exact same peptides was 16 pM when dense receptor surfaces used for initial phage display were used in assays. The phage affinity for SA-coated surfaces weakens severely toward the nanomolar regime when surface density of SA is decreased. A similarly strong dependence in this respect was observed for dendritic phage analogues. When presented with a dense SA-coated surface, dendrimer display affords up to a 10^4-fold gain in affinity over the monovalent peptide. The interplay between ligand valency and receptor density is a fundamental aspect of multivalent targeting strategies in biological systems. The perspective offered here suggests that in vivo targeting schemes might best be served to conduct ligand selection under physiologically relevant receptor density surfaces, either by controlling the receptor density placed at the selection surface or by using more biologically relevant intact cells and tissues.
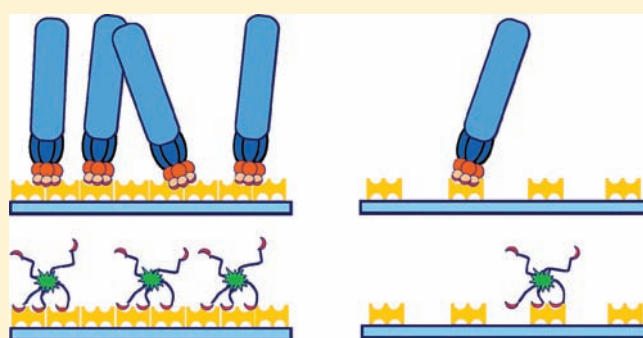
■ INTRODUCTION

Specific targeting of imaging probes or therapeutic agents to biological macromolecular structures is important for the understanding and treatment of many diseases. Design principles for multifaceted macromolecules are often based on a general concept where a multifunctional macromolecular vector is decorated with imaging groups, targeting groups, and therapeutic drugs.[1] Different types of ligands can be used as targeting moiety, with antibodies,[2] aptamers,[3] small synthetic molecules,[4] and peptides[5] being most frequently used. In recent years, target-specific oligopeptides have been identified for a wide variety of biomarkers (e.g., extracellular matrix (ECM) proteins or various cell surface receptors).[6] The major advantage of peptides over antibodies is their compact size, allowing for faster diffusion and greater tissue penetration, and ease of synthesis on a solid support.

Phage display[7] is an efficient technique to rapidly identify peptide ligands for a wide variety of targets, ranging from relatively small molecules, enzymes, and receptors,[5] to whole cells and tissues[6] and even synthetic materials.[8] Phage-display libraries are widely available, with sequence coverage (i.e., library size encoded at the DNA level) depending on the type of phage used and the length

and topology of the presented peptides. Most have been used for both in vivo and in vitro selection schemes. For oligopeptide selection, the filamentous M13 phage is often used, with the peptide sequence fused to either the pVIII or the pIII coat protein. In successive rounds of selection, elution, and amplification, new peptide binding consensus sequences can be obtained, often without knowledge of the target receptor structure.[7,9]

Selection relies heavily on multivalent ligand receptor interactions: the phage displays multiple copies of the same peptide toward a surface that may contain several receptors for binding. Because many targeting applications in the biomedical sciences rely on the monovalent peptide sequence, it is not surprising that these strategies result in disappointingly lower affinity and specificity than the original phage. One method of enhancing peptide affinity is by attaching peptides to a multivalent scaffold. A variety of scaffolds have been used to create multivalent ligands ranging in size and complexity from small organic molecules such

as oligosaccharides or cyclodextrins to dendrimers, linear polymers, micelles, liposomes, nanoparticles, and nanofibers.[10]

Our group recently introduced the concept of phage display to dendrimer display, whereby an AB_5 dendron mimics the pentavalent head of the phage.[11] In the initial design, dendrimer display featured five phage peptides appended to a pentavalent dendritic wedge via oligoethyleneoxide linkers to mimic the pentavalent architecture of the M13 phage. Individual phage peptides were introduced to this platform via native chemical ligation (NCL) at their C-terminus.[12] The platform also afforded convenient placement of a reporter group (e.g., a dye or biotin) at the focal point. The versatility in the chemical synthesis was also exploited for dendrimer display to control peptide ligand valencies, ranging from two to five (and feasibly more).[13]

Dendrimer display provides an attractive, synthetically tractable alternative to antibodies, which are more difficult to produce in large quantities. It is particularly well-suited for targeting repetitive proteinogenic nanostructures, such as collagen or other extracellular matrix (ECM) proteins. Thus, a high affinity targeting construct specific for collagen type I was developed using dendrimer display. The apparent binding affinity increased 100-fold between the synthetic pentamer and the monovalent phage peptide.[11] Nevertheless, in vitro assays demonstrated that the dendrimer-based phage mimic had a significantly lower affinity than did the corresponding phage. Here, we elucidate possible reasons for this difference.

While attractive from a biological standpoint, the heterogeneous nature and complex three-dimensional architectures[14] of the ECM may not present an ideal candidate for a more focused study on structure−function relationships with multivalent peptide ligands afforded by dendrimer display. For example, little is known about what causes the effective binding enhancement by natural multivalent constructs including phage or what molecular topologies are necessary to obtain the highest affinity for biological applications. As our approach, we use instead streptavidin (SA) as a well-defined model protein that allows detailed characterization of the factors that determine the efficacy of multivalent interactions and assess the effectiveness of peptide dendrimers as true mimics of the multivalent architecture displayed by the phage.

SA is a homotetrameric protein that contains four identical subunits, each with a high affinity biotin binding site ($K_d = \sim 10^{-14}$ M).[15] SA has been used extensively as model receptor for identifying peptide ligands through phage display, for probing the structural basis of high affinity protein−ligand interactions, and for developing and testing structure-based design strategies.[16] Screening phage peptide libraries for streptavidin have identified His-Pro-Gln (HPQ) as characteristic streptavidin-binding motif that binds in the biotin-binding site of streptavidin with a K_d of 50−150 μM, depending on the exact sequence.[17] By studying the effects of ligand valency and receptor surface density, we show conclusively that dendritic multivalent constructs display exquisitely sensitive receptor density-dependent binding affinity. Our results have important consequences for the design of multivalent targeting constructs and the general use of phage display for biomedical targeting.

■ RESULTS

To obtain an accurate comparison between the binding mechanism of the peptide-displaying phage and the corresponding peptide dendrimers, we first screened a commercially available PhD7 peptide library against streptavidin coated on polystyrene plates. After three rounds of selection and amplification, five out of six peptides displayed the HPQ motif (Table SI1) preceded by a stretch of hydrophobic residues (i.e., S, L, L, A), which is consistent with earlier phage display experiments.[16] The sequence Ser-Leu-Leu-Ala-His-Pro-Gln was selected for further use in our experiments and synthesized using tBoc-mediated solid-phase chemistry. At the C-terminus, a thioester functionality was introduced to allow NCL with the N-terminal cysteine of the wedge.[18] Because the peptides on the phage are connected to the pIII protein via a three-glycine spacer, these were also placed between the MPAL thioester and the streptavidin-binding motif. In addition to the pentavalent peptide dendrimer, which mimics the phage in valency, we also prepared divalent and tetravalent streptavidin-binding peptides by coupling the thioester-functionalized SLLA-HPQGGG peptides to AB_2, AB_4, and AB_5 synthetic wedges by NCL[11−13] (Figure 1). The synthesis of the wedges follows a previously published strategy based on dendron synthesis followed by chain extension with cystein end-capped EGs. The synthetic constructs were purified using RP-HPLC and characterized by LC−MS. As only five copies of the pIII protein are present on the head of an M13 phage, a maximum valency of five was chosen for the synthetic wedges investigated in this study.

Binding Studies with Streptavidin-Binding Peptides Using SPR and ELISA. Surface plasmon resonance (SPR) was used to investigate binding of the mono- and multivalent peptides to streptavidin.[19] The peptide constructs were injected over commercially available, SA-functionalized dextran-coated gold chips at different concentrations, ranging from 0.5−500 μM. For the monovalent peptide, the binding response was fit to a single-site Langmuir binding model, with a K_d of 120 μM. This K_d value is comparable to values reported in the literature for similar SA binding peptides peptides.[17c] Control experiments using a scrambled sequence (SALQLPHGGGC) showed no significant binding, indicating that binding is specific for the HPQ motif (Figure SI-1). The dissociation constants of the divalent, tetravalent, and pentavalent peptide constructs were measured in a similar fashion with binding responses amenable to analysis by the single-site Langmuir binding model. The multivalent peptide constructs display K_d values of 7, 5, and 1 μM for AB_2, AB_4, and AB_5, respectively, and thus all bind stronger to the streptavidin than to the monomer (Figure SI-2).[20] Although the streptavidin is in principle tetravalent, these results show that only two binding sites are active simultaneously (acting as a quasi 2D environment).

Presenting the HPQ peptide in a multivalent setting increases the binding affinity for the SA chip as compared to the monovalent peptide. The largest increase is observed for the transition from monomer to dimer. The further increase in valency toward tetramer and pentamer only slightly improves the apparent affinity and suggests that we are evaluating only the binding between the synthetic constructs and isolated SA proteins on the chip. Because the HPQ binding sites on SA are oriented in pairs, two binding sites will be available for the constructs to interact with. The monomer-to-dimer transition, therefore, gains the most in affinity enhancement. Dimer-to-tetramer or dimer-to-pentamer transition only yields an extra statistical factor.

Because phages that display the exact same peptides were selected from a large library of competitors in only three rounds of affinity selection, their K_d values for SA are expected to be much lower than 1 μM. To obtain a better insight into the phage binding behavior, we directly determined the affinity of the phage displaying the SLLAHPQ-peptide for SA. Because the macroscale dimensions of the phage do not allow analysis of SA binding
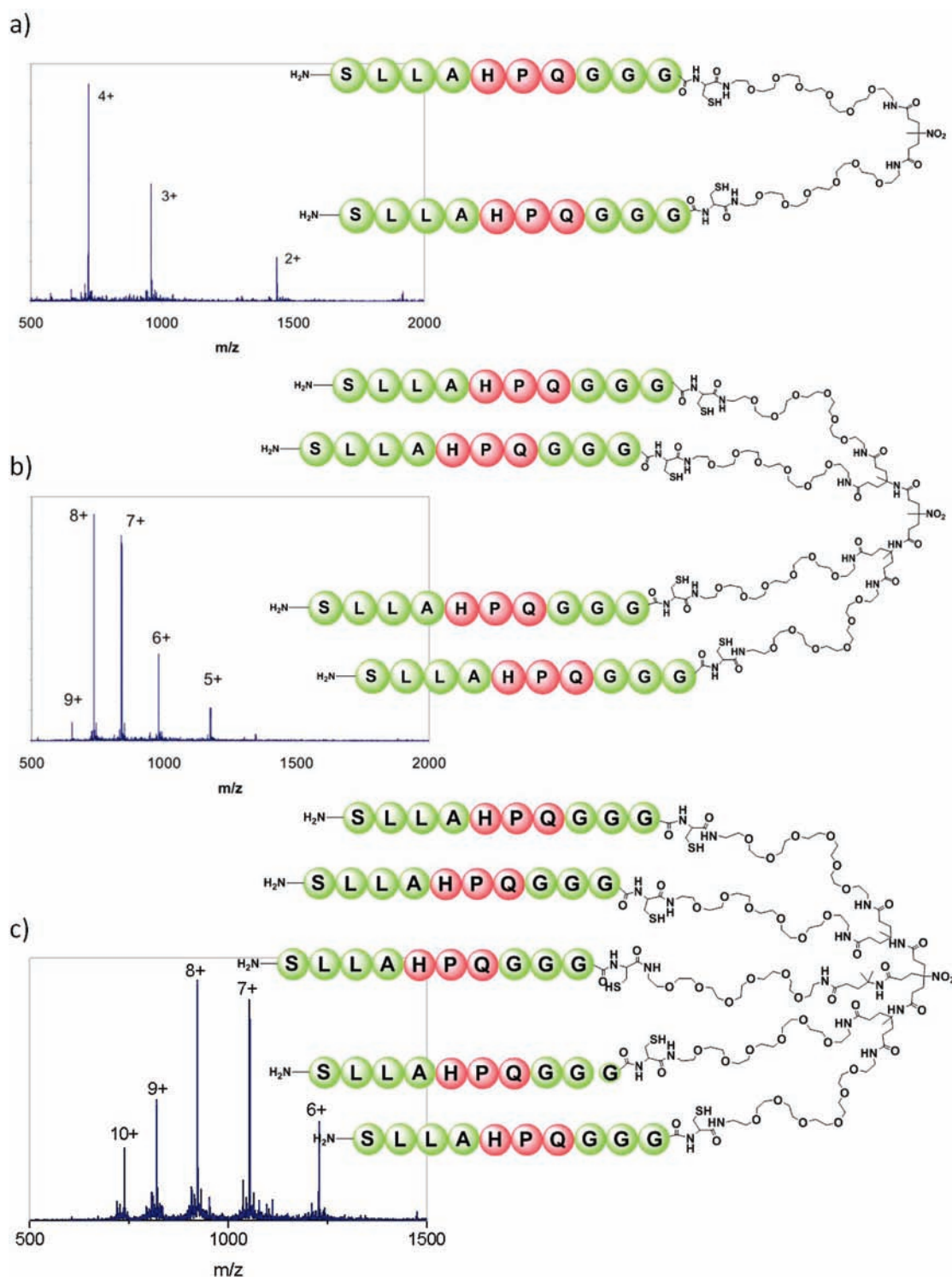
Figure 1. Structures of the (a) dimeric (MW$_{obs}$ = 2873.7 Da, MW$_{calc}$ = 2873.48 Da), (b) tetrameric (MW$_{obs}$ = 5871.09 Da, MW$_{calc}$ = 5869.82 Da), and (c) pentameric (MW$_{obs}$ = 7370.9 Da, MW$_{calc}$ = 7370.53 Da) HPQ-wedges.

using SPR, we studied binding properties to SA-coated wells using an enzyme-linked immunosorbent assay (ELISA) and compared them to the same assay for the AB$_5$ construct. A 96-well plate was coated with streptavidin, and a dilution range of the phage and AB$_5$ was incubated. Labeling with the appropriate antibody and readout of the substrate absorption yielded a binding curve that showed a K_d of 16 ± 2 pM when fitted to a

single-site binding model (Figure 2).[21] A K_d of 22 ± 3 nM, 100-fold stronger than obtained in the SPR assay, was measured for binding of the pentavalent construct on the densest SA surfaces.

The large differences between the K_d determined for the phage and the AB$_5$ binding to SA measured by ELISA and the dendritic wedges targeting SA on a Biacore chip are remarkable. However, the high density of SA when coated in these 96-well plates might
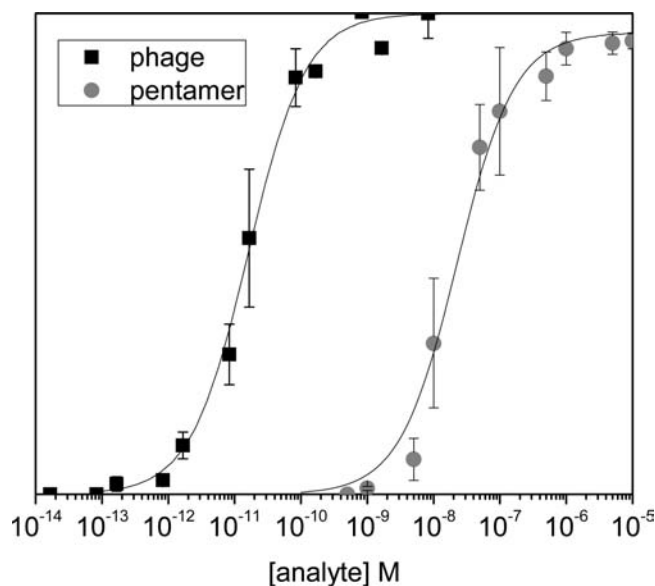
Figure 2. Solid-phase binding assay of phage SA1 (black ■) and peptide-pentamer (gray ●) on a streptavidin-coated polystyrene surface. Error bars represent ±SD. The solid line represents the fit to a single-site binding model, with a K_d of 16 pM and 22 nM for phage SA1 and peptide-dendrimer, respectively.

Figure 3. (a) SA surface coverage in % with respect to full immobilization. (b) Pentamer binding curves measured via ELISA on surfaces with various SA densities. (c) SA phage binding curves measured via ELISA on surfaces with various SA densities. (d) Overview of apparent dissociation constants of the phage, pentamer, and monomer on surfaces with different SA densities.

allow binding of the phage (and the AB_5) to multiple copies of SA simultaneously. To quantify the contribution of the effect of surface multivalency to the increased affinity, we repeated the phage-binding experiments on surfaces with different levels of SA immobilization.

Effect of Surface Density on Multivalent Binding. A series of SA surfaces were obtained by using various concentrations of SA in the coating protocol, resulting in coatings with a wide range of SA densities. To prevent protein aggregation or surface-induced clustering, samples were diluted with buffer containing small amounts of BSA. The density of SA was quantified using a biotin−HRP conjugate, revealing relative surface coverages ranging from 5% to 100% density (Figure 3a). Statistical analysis on AFM images of surfaces coated with low levels of SA showed an average interprotein distance of ∼20 nm and a homogeneous distribution of SA over the surface (Figure SI-7).

The apparent affinity of the phage was strongly dependent on the SA surface density (Figure 3b). Only the surfaces that were fully loaded with SA show picomolar affinity for SA-binding phage. A 10-fold increase in the observed K_d to 100 pM was obtained for phage SA1 when surface densities approach 80%, with further lowering of the SA density yielding concomitant declines in the affinity. An overall plot of measured dissociation constants for the various surfaces is given in Figure 3d. The limited solubility of the phage prevented measurement of phage binding curves at concentrations above 10 nM.

To allow for a fair assessment of the ability of the pentavalent dendritic wedges to mimic the phage binding properties, we also determined the binding behavior of the pentavalent peptide dendrimers on the same series of SA-coated surfaces. Comparable to the phage binding results, the synthetic multivalent phage mimic also displayed a significant receptor density-dependent binding behavior (Figure 3c). Upon decrease in surface density, the apparent binding affinity shifts from the low nanomolar regime toward the micromolar regime for the 5% covered surfaces.
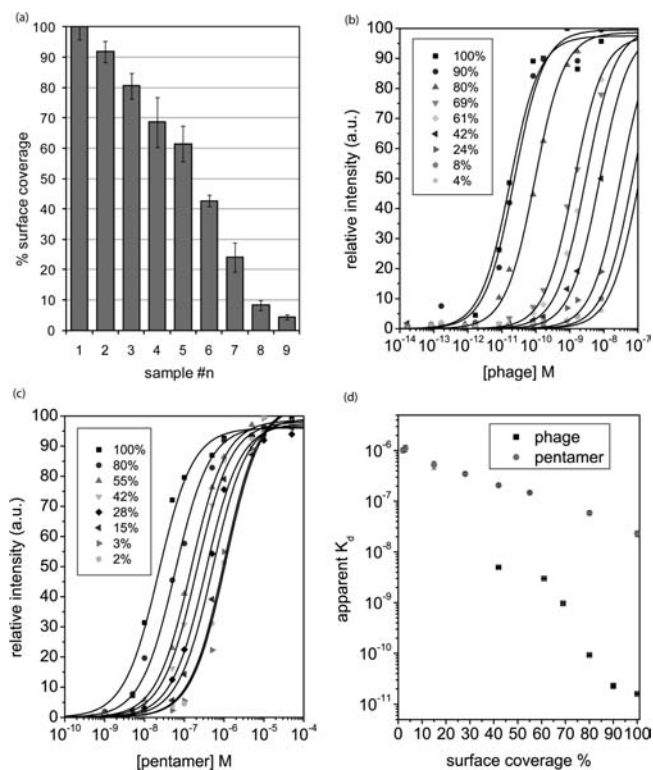
The affinity determined on surfaces with a low density of SA recapitulates the affinities obtained by SPR, indicating that in this case the multivalent peptide construct can only bind to a single SA protein. To test whether the increased affinities observed on dense SA surfaces are not due to other effects, we also measured the affinity of a monovalent peptide in the ELISA assay with a fully covered SA surface. Indeed, the obtained affinity of 97 μM (Figure SI-6) matched the affinity obtained in the SPR assay, indicative for a lack of surface density dependency. On top of the 2 orders of magnitude gain in binding affinity by using a multivalent peptide display, the multivalency effect on the surface density level accounts for an additional 2 orders of magnitude gain in affinity.

■ DISCUSSION AND CONCLUSION

Phage display is a widely used technique to identify new peptide sequences for ligand-directed targeting by selection out of a large library of competitors yielding only the strongest binders in just a few rounds of screening. Indeed, ELISA experiments indicated that the binding affinity of phage SA1 showed an impressive affinity (K_d = 16 pM) for densely coated SA surfaces. However, the individual phage peptides (SLLAHPQ) managed only weak binding (K_d = 95−120 μM), a shockingly 7-order difference in magnitude. To evaluate this phenomenon, we synthesized multivalent peptide constructs based on SLLAHPQ as mimics of the phage SA1. Dissociation constants were shown to reside in the low micromolar regime, still several orders of magnitude weaker

6639

dx.doi.org/10.1021/ja110700x |*J. Am. Chem. Soc.* 2011, 133, 6636–6641

than the original phage, but 100-fold stronger than the monovalent peptide. Besides construct valency, also surface valency was varied and shown to have striking effects on the overall binding affinities of both phage and mimics. The influence of surface density on binding affinity was analyzed using ELISA on various surface densities and showed a strong correlation between analyte density and apparent dissociation constants. Only on the densest surfaces was the phage able to bind with the picomolar affinity. Lowering the receptor concentration resulted in the affinity to drop toward the nanomolar regime. The multivalent phage mimics also showed a strong receptor density dependency. The affinity of the pentameric peptide construct for a densely coated SA surface was in the low nanomolar regime, 2 orders of magnitude stronger than the affinities measured with SPR. In total, a 10^4-fold increase from mono- to multivalent peptide display was obtained. However, the phage, displaying the exact same peptides, still binds stronger than the synthetic mimics, as presented in Figure 3d. Proposed causes hereof are the larger distance that can be spanned by the phage head as compared to the mimic and/or the preorientation of the ligands in the phage facing the binding surface that results in less entropy cost upon binding. Crystal structures of the pIII phage proteins show a distinct orientation at the phage head. Consequently, the peptides displayed here are restricted in their spacial orietation as compared to the flexible dendrons.

When using peptides identified by phage display, one should realize that the high density receptor surface used to select the phages does not resemble the natural cell membrane density of targeting receptors. Consequently, the binding behavior of the single peptide in a targeting setting might differ severely from the high phage affinity. A better choice for ligand selection therefore might be monovalent phage display. Alternatively, the selection surface in phage display can be altered to better resemble the natural receptor appearance. For successful directed targeting, both the structure and the density of the target receptor are valuable parameters that, unfortunately, are not always available.

In literature, various examples exist considering the effect of surface density on multivalent binding. Kiessling et al. previously showed the effect of receptor density on the binding affinity of antibodies, using the natural 10^6-fold stronger binding of antibodies to multivalent α-Gal epitope arrays as compared to the monovalent saccharide presentation.[22] Hereby, differences in the density of receptor-display on the surface of cell membranes caused selective cell killing. Recently, the same group showed the importance of multivalency due to TGFb-receptor assembly.[23] Huskens and co-workers investigated multivalent interactions at interfaces using molecular printboards.[24] It was shown that the binding of a divalent guest molecule on a surface is 2−3 orders of magnitude stronger than a comparable binding event in solution, originating solely from multivalency effects. Recently, Riguerra et al. published about the effect of lectin clustering on multivalent carbohydrate binding.[25] For high-density Concanavalin A surfaces, a 12-fold stronger binding of mannose-functionalized dendrimers was obtained as compared to low-density surfaces. These examples, together with our current study, show the effect of surface multivalency on binding affinities of multivalent ligands and the importance of this parameter for the design of targeting systems.

In conclusion, we have shown that not only ligand valency but also surface receptor density is an important parameter for the binding strength of both natural and synthetic multivalent constructs. A multivalent ligand presentation contributes only significantly to the overall binding affinity when the binding target displays either multiple binding sites or is present at high enough densities that multiple copies can be bound. Differences in affinity of several orders of magnitude were shown to occur for surface-based multivalent ligand—receptor interactions. Our first phage-mimic shows a comparable surface density-dependent affinity behavior as the natural phage. The remaining differences in overall binding affinity were explained by the flexible design and size of the construct and might be overcome by the use of more rigid linkers. To realistically evaluate the binding affinities of designed multivalent constructs, a surface density that matches the physiological environment should be mimicked. Vice versa, when developing multivalent targeting moieties, the density of the target receptor on the location of interest should be evaluated to optimize the design process. It has become clear that peptide sequences obtained by phage display should be used in a careful synthetic design when aiming for efficient ligand-directed targeting.

■ ASSOCIATED CONTENT

ⓢ Supporting Information. All experimental procedures, phage display assays, binding plots of scrambled and monovalent peptide control constructs, plots of the measured binding affinities by SPR of the peptide constructs, synthesis and characterization of the labeled monovalent control peptide, and AFM images and analysis of prepared SA-immobilized surfaces. This material is available free of charge via the Internet at http://pubs.acs.org.

■ AUTHOR INFORMATION

Corresponding Author
e.w.meijer@tue.nl

■ ACKNOWLEDGMENT

■ REFERENCES

(1) (a) Ringsdorf, H. *J. Polym. Sci., Polym. Symp.* **1975**, *51*, 135–153. (b) Bader, H.; Ringsdorf, H.; Schmidt, B. *Angew. Makromol. Chem.* **1984**, *123/124*, 457. (c) Kopecek, J. *Polym. Med.* **1977**, *7*, 191–221.

(2) Damle, N. K.; Frost, P. *Curr. Opin. Pharmacol.* **2003**, *3*, 386–390. Maison, W.; Frangioni, J. V. *Angew. Chem., Int. Ed.* **2003**, *42*, 4726–4728.

(3) (a) Hermann, T.; Patel, D. J. *Science* **2000**, *287*, 820. (b) Bagalkot, V.; Farokhzad, O. C.; Langer, L.; Jon, S. *Angew. Chem., Int. Ed.* **2006**, *45*, 8149. (c) Osborne, S. E.; Matsumura, I.; Ellington, A. D. *Curr. Opin. Chem. Biol.* **1997**, *1*, 5–9.

(4) Reddy, J. A.; Low, P. S. *Crit. Rev. Ther. Drug Carrier Syst.* **1998**, *15*, 587–627.

(5) Arap, W.; et al. *Nat. Med.* **2002**, *8*, 121–127.

(6) Ruoslathi, E.; Bhatia, S. N.; Sailor, M. J. *J. Cell Biol.* **2010**, *188*, 759–768.

(7) Scott, J. K.; Smith, G. P. *Science* **1990**, *249*, 386–390.

(8) (a) Sanghvi, A. B.; Miller, K. P.-H; Belcher, A. M.; Schmidt, C. E. *Nat. Mater.* **2005**, *4*, 496–502. (b) Whaley, S. R.; English, D. S.; Hu, E. L.; Barbara, P. F.; Belcher, A. M. *Nature* **2002**, *405*, 665–668. (c) Serizawa, T.; Sawada, T.; Matsuno, H.; Matsubara, T.; Sato, T. *J. Am. Chem. Soc.* **2005**, *127*, 13780–13781. (d) Serizawa, T.; Sawada, T.; Kitayama, T. *Angew. Chem., Int. Ed.* **2007**, *46*, 723–726.

(9) (a) Smith, G. P.; Petrenko, V. A. *Chem. Rev.* **1997**, *97*, 391–410. (b) Pasqualini, R.; Ruoslahti, E. *Nature* **1996**, *380*, 364–366. (c) Bass, S.;

Greene, R.; Wells, J. A. *Proteins* **1990**, *8*, 309–314. (d) Sidhu, S. S. *Biomol. Eng.* **2001**, *18*, 57–63. (e) Devlin, J. J.; Panganiban, L. C.; Devlin, P. E. *Science* **1990**, *249*, 404–406. (f) Katz, B. A. *Annu. Rev. Biophys. Biomol. Struct.* **1997**, *26*, 27–45.

(10) (a) Kiessling, L. L.; Gestwicki, J. E.; Strong, L. E. *Angew. Chem., Int. Ed.* **2006**, *45*, 2348. (b) Mammen, M.; Choi, S.-K.; Whitesides, G. M. *Angew. Chem., Int. Ed.* **1998**, *37*, 2755–2794. (c) Reulen, S. W. A.; Dankers, P. Y. W.; Meijer, E. W.; Merkx, M. *J. Am. Chem. Soc.* **2009**, *131*, 7304–7312. (d) Kim, Y.; Zimmerman, S. C. *Curr. Opin. Chem. Biol.* **1998**, *2*, 733. (e) Torchilin, V. P. *Nat. Rev. Drug Discovery* **2005**, *4*, 145. (f) Lusvarghi, S.; Kim, J. M.; Creeger, Y.; Armitage, B. A. *Org. Biomol. Chem* **2009**, *7*, 1815–1820. (g) Kane, R. S. *AIChE J.* **2006**, *52*, 3638–3644. (h) Cui, H.; Webber, M. J.; Stupp, S. *Biopolymers* **2010**, *94*, 1–18. (i) Ma, H.; Zhou, B.; Kim, Y. S.; Janda, K. D. *Toxicon* **2006**, *47*, 901–908.

(11) Helms, B. A.; Reulen, S. W. A.; Nijhuis, S.; de Graaf-Heuvelmans, P. T. H. M.; Merkx, M.; Meijer, E. W. *J. Am. Chem. Soc.* **2009**, *131*, 11683–11685.

(12) Dawson, P. E.; Muir, T. W.; Clark-Lewis, I.; Kent, S. B. H. *Science* **1994**, *266*, 776–779.

(13) Lempens, E. H. M.; Helms, B. A.; Bayles, A. R.; Merkx, M.; Meijer, E. W. *Eur. J. Org. Chem.* **2010**, 111–119.

(14) (a) Vakonakis, I.; Campbell, I. D. *Curr. Opin. Cell Biol.* **2007**, *19*, 578. (b) Gelse, K.; Poschl, E.; Aigner, T. *Adv. Drug Delivery Rev.* **2003**, *55*, 1531. (c) Brodsky, B.; Ramshaw, J. A. M. *Matrix Biol.* **1997**, *15*, 545.

(15) Green, N. M. *Methods Enzymol.* **1990**, *184*, 51–67.

(16) (a) Chaiet, L.; Wolf, F. J. *Arch. Biochem. Biophys.* **1964**, *106*, 1–5. (b) Wilchek, M.; Bayer, E. A. *Avidin-Biotin Technol.* **1990**, 3–45. (c) Sano, T.; Cantor, C. R. *Proc. Natl. Acad. Sci. U.S.A.* **1990**, *87*, 142–146. (d) Weber, P. C.; Ohlendorf, D. H.; Wendoloski, J. J.; Salemme, F. R. *Science* **1989**, *243*, 85–88. (e) Green, N. M. *Adv. Protein Chem.* **1975**, *29*, 85.

(17) (a) Katz, B. A. *Biomol. Eng.* **1999**, *16*, 57–65. (b) Katz, B. A. *Biochemistry* **1995**, *34*, 15421–9. (c) Chang, Y.-P.; Chu, Y.-H. *Anal. Biochem.* **2005**, *340*, 74–79.

(18) Hackeng, T. M.; Griffin, J. H.; Dawson, P. E. *Proc. Natl. Acad. Sci. U.S.A.* **1999**, *96*, 10068–10073.

(19) Lofas, S.; Malmqvist, M.; Ronnberg, I.; Stenberg, E.; Liedberg, B.; Lundstrom, I. *Sens. Actuators, B* **1991**, *5*, 79–84.

(20) All obtained dissociation constants display a typical error margin of 10−25%.

(21) From the phage titer, the stock concentration of phages is determined in plaque-forming-units (pfu)/mL. Because one phage is needed to produce a single pfu, the concentration of phages in mol/L can be deduced from pfu/mL by conversion to pfu/L and division by Avogadro's number. Barbas, C. F.; Burton, D. R.; Scott, J. K.; Silverman, G. J. *Phage Display: A Laboratory Manual*; Cold Spring Harbor: Plainview, NY, 2001.

(22) Carlson, C. B.; Mowery, P.; Owen, R. M.; Dykhuizen, E. C.; Kiessling, L. L. *ACS Chem. Biol.* **2007**, *2*, 119–127.

(23) Li, L.; Orner, B. P.; Huang, T.; Hinck, A. P.; Kiessling, L. L. *Mol. BioSyst.* **2010**, *6*, 2392–2402.

(24) (a) Huskens, J.; Mulder, A.; Auletta, T.; Nijhuis, C. A.; Ludden, M. J. W.; Reinhoudt, D. N. *J. Am. Chem. Soc.* **2004**, *126*, 6784–6797. (b) Huskens, J. *Curr. Opin. Chem. Biol.* **2006**, *10*, 537–543. (c) Mulder, A.; Auletta, T.; Sartori, A.; Del Ciotto, S.; Casnati, A.; Ungaro, R.; Huskens, J.; Reinhoudt, D. N. *J. Am. Chem. Soc.* **2004**, *126*, 6627–6636.

(25) Munoz, E. M.; Correa, J.; Fernandez-Megia, E.; Riguerra, R. *J. Am. Chem. Soc.* **2009**, *131*, 17765–17767.